MOL2NET, **2022**, 7, **ISSN**: 2624-5078
https://mol2net-07.sciforum.net/

MOL2NET'21, Conference on Molecular, Biomedical & Computational Sciences and Engineering, 7th ed.

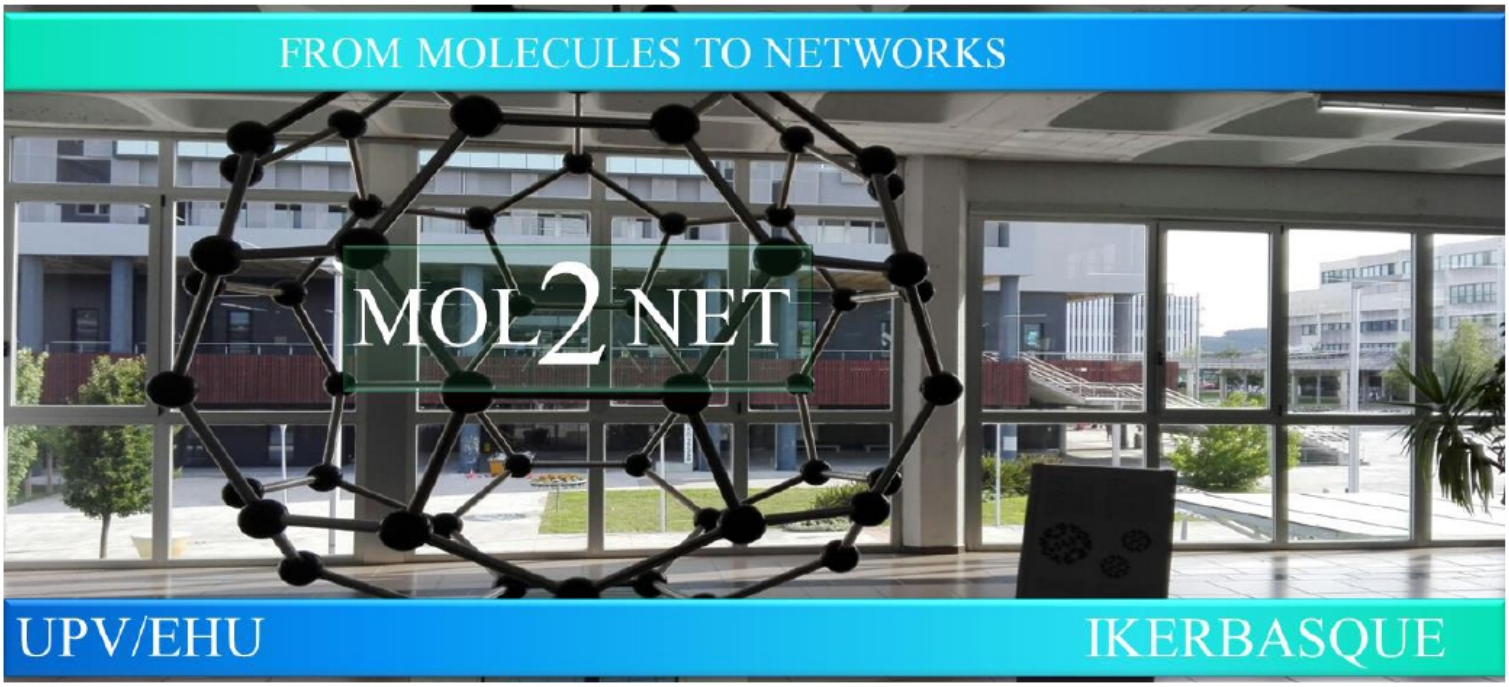

Optimization Of Robotic P-Gtaw Welding Process Parameters For Welding Ni-Cr Steel Alloy By Combining A Deep Neural Network And Multi objective Genetic Algorithm

Aned Esquerra-Arguelles[1] | Alberto Martínez Noa[2]

[1]Postgraduate in Systems Engineering, Universidad Autonoma de Nuevo Leon, Nuevo Leon, Mexico
[2]CIDET, Autonomous University of Nuevo Leon, San Nicolas de las Garza, Mexico

Correspondence
Aned Esquerra-Arguelles, Postgraduate in Systems Engineering. Nuevo Leon. Mexico.
Email: aned.esquerrargls@uanl.edu.mx

Summary

NSGA-type algorithms are widely use in mathematical and operations optimization to create diverse strategies for hyper-heuristics and heuristics methodologies in problem solving, in critical welding

KEYWORDS:
Neural networks, P-GTaw Welding, NSGA

1 | INTRODUCTION

Tungsten inert gas (TIG) welding became an overnight success in the 1940s for joining magnesium and aluminium. In the TIG welding process, the arc is formed between a pointed tungsten electrode and the workpiece in an inert atmosphere of argon or helium. The small intense arc provided by the pointed electrode is ideal for high quality and precision welding. Because the electrode is not consumed during welding, the TIG welder does not have to balance the heat input from the arc as the metal is deposited from the melting electrode [1]. The development of robotic in arc welding technology has widely diversified in terms of design and modelling, control system and sensing ability [2] [3]. According to Hussin et al [4], the developments in robotics application are affected by a lot of factors such as speed, flexibility, mobility, compactness, navigation, localization, and mobile platform. Besides, such robotic systems can be controlled by a complicated neural network brain. The optimization process involves mathematical techniques that try to simplify a physical phenomenon or industrial process with a specific goal. The main purpose of such techniques is that measurable variables can be managed to optimize it (ex. reduce defects). In the case of welding, Cruz et al [5], suggested that three main optimization techniques (Taguchi, surface response and genetic algorithms) were employed to optimize the welding process.

The welding variables or inputs are well defined in welding codes since they have a significant impact on their mechanical properties. Nowadays, application of design of experiment (DOE), evolutionary algorithms and computational network are widely used to develop a mathematical relationship between the welding process input parameters and the output variables of the weld joint to determine the welding input parameters that lead to the desired weld quality [6]. In that sense, optimization processes are well focused on automatic and robotized welding since they are employed in companies where its main purpose is generating profits. The above since such techniques tends to reduce waste through maximization of productivity [7].

Cruz et al [8], optimized a mechanized GTAW process of 5mm thickness Ti6Al4V sheets. The authors employed the surface response methodology to optimize the welding Charpy impact toughness. The results suggest that by employing parameters such as 141 A, 10 V and 99.9 mm.min-1 of welding speed a 10 J toughness can be achieved. Marroquin et al [9], employed a sequential surrogate-based multi-objective optimization method for the initial data set of GTAW welding. The results, suggests that the method was able to identify solutions on or very close to the true Pareto Front and that was no statistical significance

when different data set were employed.

Magudeeswaran et al [10], presented an optimization of process parameters of the activated tungsten inert gas welding for aspect ratio in a UNS S32205 (duplex stainless steel) welds. The authors, performed a Taguchi orthogonal array (OA) experimental design and other statistical tools such as Analysis of Variance (ANOVA) and Pooled ANOVA techniques to optimize weld width, penetration depth and aspect ratio. The results, suggests that the optimum response can be found at a 1 mm electrode gap, 130 mm/min travel speed, 140 A current and 12 V voltage.

Pamnani et al [11], performed optimization of A-GTAW welding parameters for a DMR 249A naval steel. The optimization was focused on the deep penetration (DOP) enhancement through surface response methodology (RSM) and the Taguchi technique. The results suggested, that the maximum DOP can be obtained at 300A, 60 mm.min-1 weld speed and 4mm of arc gap. Sathiya et al [12], performed optimization of welding parameters for laser bead-on-plate welding using the Taguchi method. The analyzed variables were beam power, travel speed and focal position to optimize the two responses (bead width and depth of penetration). The optimization results were evaluated through the microstructural characterization and hardness measurements across the weld zone.

Jing-Shiang and co-authors [13], developed a principal component analysis for multiple quality characteristics optimization MIG welding. In that sense, the Taguchi method was employed to analyze weld variables such as filler metal, MIG current, welding speed, among others. The results suggest, that the optimum micro-hardness and bending strength was obtained when 5356 filler metal, 100 A, 80mm.min-1 welding speed, 1.7 mm of workpiece gap, 50° arcing angle and 20° of groove angle.

Lostado-Lorza and co-workers [14], developed a design and optimization of welded products by employing genetic algorithms (for adjusting the finite element models and reduce computational cost). As the welded product becomes more complex, residual stresses and strains are more difficult to obtain and predict as they depend greatly on the sequence of its manufacture process. The results showed, that the combination of finite element, genetic algorithms and model trees can be successfully employed for the design and optimization of complex welded products.

Tansel et al [15], performed optimizations of friction stir welding of aluminium alloy by employing of genetically optimized neural network. In the work mentioned before, a tool speed that ranges from 500-1500 rpm and a welding speed ranging from 6.25-20 mm.min-1were employed as input variables while elongation, tensile and yield strength were the system responses. The genetically optimized neural network system results revealed, that after 1160 iterations with optimal tool speed and the feed rates (1406 rpm and 19.9 mm.min-1 respectively) the tensile strength estimation was reduced (from 112 to 80 MPa) when the acceptable elongation range was narrowed.

Kondapalli et al [16], optimize the fusion zone grain size (GS), Vickers hardness (HV) and ultimate tensile strength (UTS) in a welded AISI 304 L stainless steel employing genetic algorithms (GA). The results, suggests that the Pulsed Current Microplasma Arc Welding optimal parameters were a 4-7 A, 40 pulses.s-1 and 50% of the pulse width. The parameters mentioned above yielded responses about 201 HV, 20.05 microns of GZ and 789 MPa of UTS; the difference between the GA prediction and experimental values ranged from 0.02 to 0.3% for UTS and HV. On the contrary, the GZ yielded a difference of about 10% in comparison to the experimental values. Another optimization works can be founded on the following literature [17] [18] [19].

Perez-Pozo et al [20], performed optimization of robotized welding parameters (MIG) for the recovery of Pelton turbine blades (made of SAE 4140 steel). Parameters, such as voltage (V), welding speed (S), swinging length (L), welding speed (S), wire-speed (W) and gas flow rate were analyzed by mathematical models, genetic algorithms and metallography. The results suggest that the increase in the voltage in the process tends to flatten the welding bead in the low-slope zones, thus increasing the width; zones with more inclined slopes behave oppositely, and the welding heights are increased by run-off. An excessively high voltage can cause porosity, sprinkling, and erosion depending on the inclination in the process. As the welding speed increases, the quantity of thermal energy via the welding length transferred from the arc to the base metal decreases because the arc acts directly on the base metal.
The aim of this work is to present the pulsed Gas Tungsten Arc Welding (P-GTAW) process optimization by using a new

approach combining a deep neural network and a multi-objective genetic algorithm to find the optimal values of three process key variables.

2 | MATERIALS AND METHODS

2.1 | Base material and welding wire

The weldments were prepared from two steel sheet made of Ni-Cr steel of 110×110×4.0 mm. The Ni-Cr steel has a tensile strength of 1252±6.48 MPa, a yield strength at 0.2% of 790±11.50 MPa and 10.28±0.63% of elongation. The Ni-Cr chemical composition is depicted in Table 1. The filler metal, employed within this experiment was an AWS A 5.18: ER70S-6 of 0.86 mm diameter. The equivalent carbon (Eq. C), shown in Table 3 was calculated based on the formula published in the following reference [21].

TABLE 1

Ni-Cr Steel	C	Ni	Mn	Cr	Si	Mo	P	S	Eq.C
	0.27	1.82	1.34	0.53	0.42	0.54	0.015	0.003	0.86

2.2 | Joint design and welding of test coupons

In this work, a squared-groove butt joint was employed, both butting members had 2 mm of root opening. The welding strategy was performed by following the data shown in Table 2. A Fanuc F118718 ArcMate 120IC robotic arm was employed to move a Fronius 23275771 GTAW welding machine. An open flame torch, with propane as fuel, was employed to preheat welding coupons. The GATW welding machine has an EWTh-2 3.2 mm diameter electrode, a 12mm internal diameter torch and the argon (99.99% purity) gas flow was about 16.70 cm3.s-1. Figure fig:equipos, shows the robotic arm-GTAW welding machine configuration. Thirty-one test coupons of square groove weld were manufactured, then were visually inspected to evaluate weld soundness. Finally, test coupons were cleaned and marked (see Figure fig:cupones).

FIGURE 1 GTAW welding test coupons

2.3 | Mechanical testing of test specimens

After test coupons were finished, the mechanical testing was performed on two test specimens taken from them. The test specimens were cut on a Supreme ® water jet machine, then machined until the final dimensions on a VF-2 CNC Hass machine.

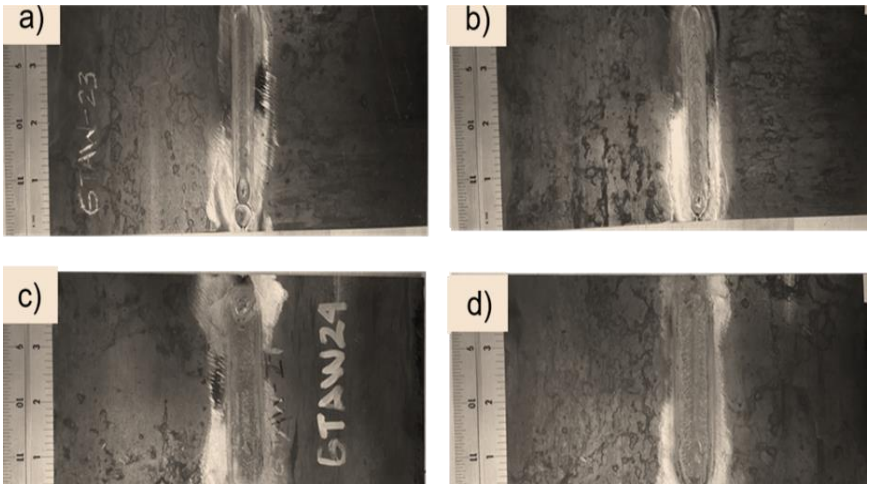

FIGURE 2 Welding equipment configuration on FANUC robotic arm

The above, until they fulfilled the ASTM E8 standard sub size (6 mm width) test specimens dimensions. The width, gage length and thickness of the tests specimens were measured with a calliper of 0.001 mm resolution. Once test specimens were properly machined, they were mounted on the knurled flat grips of an INSTRON 4482 testing machine (0.01kN resolution). The speed of testing to determine tensile properties was about 15 mm.min-1, then the broken specimens were put together to measure the gage length after a fracture. Two test specimens were tested and averaged and its average registered in Table 2.

2.4 | Mathematical model

This section presents one mathematical formulation using a feed-forward artificial neural network to represent the problem of study.

$$f(X,W) = \gamma_3\left(\sum_{z=1}^{\theta} w_z^3 \gamma_2\left(\sum_{j=1}^{\rho} w_{jz}^2 \gamma_1\left(\sum_{i=1}^{\mu} x_i w_{ij}^1 + w_{\mu+1,j}^1\right) + w_{\rho+1,j}^2\right) + w_{\theta+1}^3\right) \tag{1}$$

The X comprises the variables involved in the analysis of the process, see Table factores, W represents the weights of neurons in each layer, γ_k the current activation function in subsequent levels, k represents the number of hidden layers, θ, ρ, μ represent the amount of synapses or links between neurons to the next layer.

Thus, the optimization model can be written as follows:

$$\text{Max Tensile Strength:} \quad f_1(A,T,H_z,T_o) \tag{2}$$
$$\text{Max Elongation:} \quad f_2(A,T,H_z,T_o) \tag{3}$$
$$\text{subject to:} \quad A \in [A^{\min}, A^{\max}] \tag{4}$$
$$T \in [T^{\min}, T^{\max}] \tag{5}$$
$$H_z \in [H_z^{\min}, H_z^{\max}] \tag{6}$$
$$T_o \in [T_o^{\min}, T_o^{\max}] \tag{7}$$
$$\tag{8}$$

TABLE 2 Factors and levels for the design of experiments

Symbols	Factors	Levels	
		-1	1
A	Current (A)	200	300
T	Temperature (ºC)	25	150
H_z	Frequency (Hz)	20	50
T_o	Torch speed (mm.min^{-1})	180	450

2.5 | GA algorithm validation run and testing

To validate the GA algorithm, three test coupons were manufactured with the same materials described in 2.1. The manufacturing procedure was similar as mentioned in 2.3.1 and the parameters stated in Table 3. Then, mechanical testing test specimens were manufactured and tested accordingly to 2.3.2.

3 | SOLUTION METHOD

Figure fig:diagrama$_f lujoshowstheprocedureofthesolutionmethod.Thismethodologyconsistsof fivesteps$:

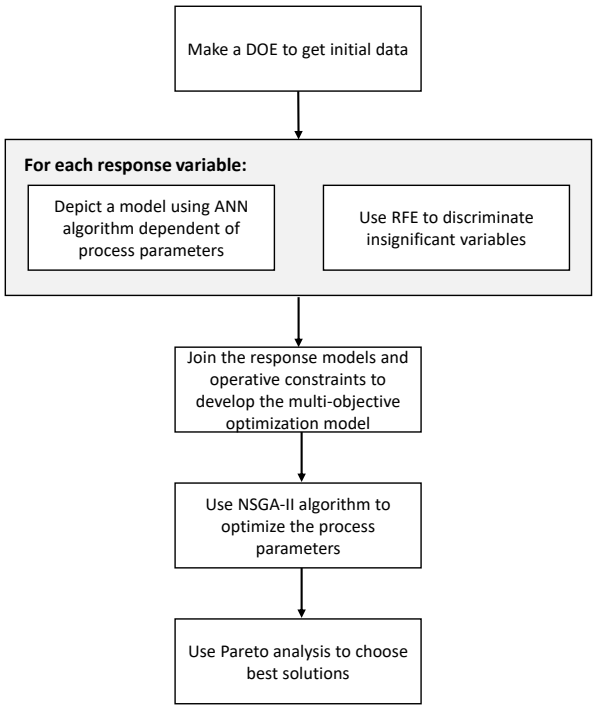

FIGURE 3 Methodology used to propose solutions

1. First, a DOE over process parameters is developed. Each treatment of DOE is a configuration of process parameters. Response variables are the corresponding quality measures of shear load and remaining fiber.

2. Each objective function is represented with a feed-forward artificial neural network of several hidden layers (obj:shear$_l oad, obj$: $remaining_f iber).Then, thebest - fittingparameters forthemodelare foundusingaCross - validationRecursiveF$

The selected solutions represent a set of engaged ones, fitted from DOE collected data. The ANN models of the objective functions allow analyzing unexplored solutions without performing more physical tests.

3.1 | NSGA-II

The Nondominated Sorting Genetic Algorithm (NSGA-II) was first presented by Deb et al[1]. As many classic genetic algorithm variations the NSGA-II begins with the generation of a subset of feasible solutions, the initial population. Then, the main procedure is repeatedly executed to produce the necessary number of generations to evolve. Starting from a population P_t, an offspring of the previous one Q_t is generated using cross-over and mutation strategies. The following step is to select a set of individuals $R_t = P_t \cup Q_t$ is discriminated into subsets called fronts ($F_1, F_2, \dots$) using a non-dominated sorting procedure, where F_1 is the set of non-dominated solutions, F_2 is the set of solutions only dominated by solutions in F_1 and so on. The first front of each generation is included in the new population P_{t+1}. When a front does not fit entirely into P_{t+1}, its solutions are sorted using a crowding distance procedure, and the first most dispersed solutions are selected. In this way, a new population has been emerged and a fresher generation has been completed. Figure fig:nsga2 shows the algorithm strategy.

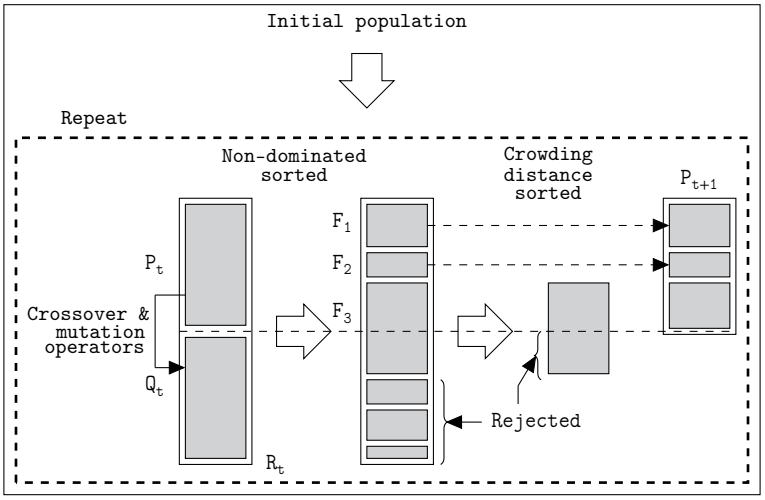

FIGURE 4 NSGA-II procedure

A feasible solution from the initial population is built uniformly by selecting randomly items in the interval of variables $[O^{\min}, O^{\max}]$.

The cross-over strategy takes the variable values from two parents and inherits the relation of these values as follows: the value of variable O is randomly selected from interval composed by the values this variable in its parents.

The mutation strategy consists on selecting randomly a variable to mutate. The value is set randomly from possibles value choices. If the variable is O, the value is randomly selected in the interval $[O^{\min}, O^{\max}]$.

4 | DATA COLLECTING

4.1 | Experimental details

4.2 | Specimens preparation

The evaluation specimen preparation was carried out under standard conditions[2]. Initially, different test coupons were prepared via adhesive join of two plates; one of 6061-T6 anodized aluminum alloy (153x102x6 mm) and the other of unidirectional carbon fiber laminate (153x102x3.9 mm). The laminates were joined by means of an adhesive layer, which was poured over a proportional area to the overlap length (predictor variable) and coupon width. To improve adhesion, both plates were pressed using a 0.120 MPa pressure. Prior curing, the adhesive excess was removed with a spatula while excess generated at the edges

was spread over them to form a fillet. The adhesive thickness was verified by an optical comparator (thicknesses of 190-230 μm). For the adhesive application, a dispenser gun (in which the adhesive cartridge and the dispenser nozzle were mounted), was used. Prior to adhesive application, pouring of about 50 g of adhesive was used to purge the cartridge. In this manner, it was ensuring that the air bubbles were removed from the adhesive blend and therefore a homogeneous blend was obtained. Finally, the test coupons were water-jet cut, in order to obtain standard specimens of 25.4 ± 0.05 mm wide. In addition, to compensate for the moment generated by the thickness difference between substrates, tabs were glued at the end of every test specimen. The diagram for test specimens is displayed in Figure fig:specimen.

5 | RESULTS

The proposed methodology is implemented in the R language[3] (version 3.5.2). A computer with a Windows 7x64 operating system, Intel Xeon 3.4 GHz CPU E3-1245 v3 @ 3.4GHz 3.40 GHz processor, and 16 GB of RAM is used.

5.1 | Visual inspection

After the GTAW welding process was performed, the test coupons were visually inspected (VI) to find welding defects. The visual inspection reveals that 32% of the test coupons had welding discontinuities, such discontinuities were classified following AWS B1.11 [23] guide and the following reference [21]. In that sense, 19% of the discontinuities were classified as underfill (UF), 6.5% classified as undercut (UC) and finally, 6.5% was identified as lack of fusion (LF). The results showed in Table 2, suggests that the LF occurs at low coupon temperatures a (25°C) and higher torch speed (480mm.min-1); the tensile strength and welding are reduced significantly (45 and 39% respectively) in comparison to base metal values (see 2.1). A similar trend is depicted for the UC, but the reduction was about 5% of the base metal values for tensile strength. Finally, for the UF seems that the higher torch speed (480mm.min-1) has the highest influence in the generation of such discontinuity and a reduction of about 70% for both the tensile strength and elongation. The reduction in mechanical properties are related to the depth of every discontinuity, while the LF ranges from 0.5 0.8mm (for test coupons 221 and 3030 respectively) the UF reaches about 2mm (for test coupons 12, 13, 15 and 25). On the other hand, the UC had the lowest depth that was lesser than 0.2mm (for test coupons 26 and 28). The rest of the test specimens did not reveal any welding discontinuities or base metal defects on its surface.

5.2 | Tensile strength and elongation values

Table 2, shows the mechanical testing results (tensile strength and elongation) for every test coupon as well as its standard deviation. The results suggest that the test specimens taken from test coupons (TC) number 19, 23 and 24, had tensile strength and elongation values higher than the ones reported by base metal (see 2.1). The rest of the test coupons (except the ones mentioned in 3.1), yield efficiency that ranges from 75 95% for tensile strength.

References

1. Deb Kalyanmoy, Pratap Amrit, Agarwal Sameer, Meyarivan TAMT. A fast and elitist multiobjective genetic algorithm: NSGA-II. *IEEE transactions on evolutionary computation.* 2002;6(2):182–197.

2. ASTM International . D1002-10: Standard Test Method for Apparent Shear Strength of Single-Lap-Joint Adhesively Bonded Metal Specimens by Tension Loading (Metal-to-Metal). 100 Barr Harbor Drive, PO Box C700, West Conshohocken, PA 19428-2959. United States2001. ASTM International.

3. R Core Team . R: A Language and Environment for Statistical Computing. R Foundation for Statistical ComputingVienna, Austria2017.

ORCID

Aned Esquerra-Arguelles https://orcid.org/0000-0003-1448-0407
Alberto Martínez Noa https://orcid.org/0000-0002-3641-1245